



## Prediction of Time-series Friction Data using ANFIS

Cem Korkmaz<sup>1,\*</sup>, İlyas Kacar<sup>2</sup>

<sup>1</sup>Çukurova University, Faculty of Agriculture, Department of Agricultural Machinery and Technology Engineering, Adana, Türkiye

<sup>2</sup>Niğde Ömer Halisdemir University, Engineering Faculty, Department of Mechatronics Engineering, Niğde, Türkiye

### HIGHLIGHTS

- ANFIS model optimised friction data for peanut grading machines.
- Simulation using DEM took 63 days for 60 seconds of real-time data.
- Peanut classification model achieved a correlation of 0.798854.
- ANFIS eliminates data pre-processing and enhances performance.

### Abstract

Modelling is frequently used in science and industry. Friction, wear, and corrosion issues are the main design criteria in peanut kernel grading machines. In this study, the time-series of friction force data is modelled with adaptive neuro-fuzzy inference system (ANFIS). Machine learning focuses on developing models for prediction and classification without explicit programming. The data on the friction force is obtained from a simulation based on the discrete element method. The simulation takes 63 days, 18 hours and 27 minutes to calculate the real time of 60 seconds. A Takagi-Sugeno type ANFIS network is constructed. The network is clustered using grid partitioning method. ANFIS helps to optimise machine performance by modelling friction data. In the obtained peanut kernel classification model, the correlation value is 0.799 and the root of the mean square error is 0.514 N. The percentage of the mean absolute error is found to be 1.666%. 100 iterations are run. Calculations take 20.7 seconds. The model has a high linear relationship. It is also observed that the ANFIS network eliminates the need for any pre-processing of the data. Background of the network used, its hyper-parameters, and the prediction performance are presented in the study.

**Keywords:** Peanut kernel classification; discrete element method; adaptive neuro-fuzzy inference system; modelling; prediction

### 1. Introduction

Modelling is a well-established and effective tool widely used in science and industry. It is based on the functions in mathematics. Words such as 'prediction', 'estimation', 'insight', 'foresight', or 'intuition' can be used to explain the task of a model. Curve fitting, simulation, and artificial intelligence are frequently used for

**Citation:** Korkmaz C, Kacar İ (2025). Prediction of time series friction data using ANFIS. *Selcuk Journal of Agriculture and Food Sciences*, 39(1), 121-134. <https://doi.org/10.15316/SJAIFS.2025.011>

\*Correspondence: [ckorkmaz@cu.edu.tr](mailto:ckorkmaz@cu.edu.tr)

Received date: 24/12/2024

Accepted date: 17/02/2025

Author(s) publishing with the journal retain(s) the copyright to their work licensed under the CC BY-NC 4.0.

<https://creativecommons.org/licenses/by-nc/4.0/>

modelling. In this study, the words 'network' and 'model' are used in the same mean because there are function(s) behind a network, as well.

Machine Learning (ML) is a rapidly developing technique that focuses on the development and implementation of algorithms and codes that allow computers to learn from data and make predictions or decisions without explicit programming. It has attracted great interest in recent years due to its ability to predict, classify, and solve complex problems in almost all fields. ML techniques can be generally categorized as supervised, unsupervised, or reinforced learning approaches (Brockwell and Davis 2002). Supervised learning requires training before predicting or classifying. Unsupervised learning needn't to be trained initially. Its training takes place in the realm of working condition. Reinforcement learning focuses on training before usage (Sutton RS 2018). Advances in ML algorithms have accelerated due to the availability of large datasets, increased computing power, and improvements in algorithmic frameworks. Deep learning techniques such as Convolutional Neural Networks (CNNs) and Recurrent Neural Networks (RNNs) have emerged as powerful models for image recognition, Natural Language Processing (NLP), speech recognition, and other complex tasks (LeCun et al. 2015). Transfer learning has also gained importance as it allows fine-tuning of pre-trained models on large datasets to specific applications with limited data (Pan and Yang 2009). In addition, interpretations that provide information on how models make predictions or judgements are also increasing interest in ML methods. These efforts aim to address concerns about model reliability and accuracy (Caruana et al. 2015). Time-series analysis is a fundamental technique used in a variety of disciplines to understand and analyze data collected over time (Murphy 2022). Time-series data can be found in fields as diverse as finance, economics, environmental science and engineering. In the analysis of time-series, many more sophisticated modelling techniques are often used, such as Autoregressive Integrated Moving Average (ARIMA), exponential smoothing methods, state space models, and RNN. In recent years, there have been significant developments in time-series analysis methods. ML algorithms have been included in traditional time-series models to improve forecasting performance. Researchers have investigated the use of deep learning techniques such as Long Short-Term Memory (LSTM) networks to model complex temporal patterns (Lipton 2015). Furthermore, attention mechanisms have been used to improve the interpretability of the model by highlighting important features (Chen and Shi 2021). Another emerging trend is to hybridize single models to obtain more accurate forecasts. Adaptive Network Based Fuzzy Inference System (ANFIS) is one of the popular hybrid methods. It combines the fuzzy logic and neural networks to create the hybrid model so that it can effectively handle uncertainty and non-linearity in data. This approach has attracted great interest in various fields, including control systems, pattern recognition, and decision-making processes (Jang and Sun 1995). While an ANFIS model uses the concept of fuzzy clusters and fuzzy rules to represent linguistic variables and the relationships between them, its neural network part helps to adapt the parameters of these fuzzy rules to the input-output data pairs. The adaptive nature of ANFIS allows it to learn iteratively from the data and thus perform accurate modelling and prediction. Recent research has focused on improving the capabilities of ANFIS models through various techniques such as optimization algorithms (Khalaf et al. 2024; Tien Bui et al. 2018). For example, evolutionary algorithms such as genetic algorithms have been used to optimize the learning process by searching for optimal hyper-parameters that minimize the error between predicted and actual outputs (Chou et al. 2020). Furthermore, hybrid approaches combining ANFIS with other ML techniques such as support vector machines or deep learning architectures have been proposed to improve model performance (Irshaid and Abu-Eisheh 2023). These developments aim to improve the accuracy, interpretability and efficiency of ANFIS models to address complex real problems.

Discrete Element Method (DEM) is a simulation technique used to simulate the interaction between solid particles and their environment. It has attracted great interest in recent years thanks to its ability to calculate complex interactions between individual particles. DEM is widely applied in various fields such as geotechnical engineering, energy, chemical, mining, pharmaceuticals, agriculture and food processing (Zhang et al. 2024; Zhou et al. 2024). The method involves in analysing every single particle by calculating its motion based on contact forces and other multi-physics, taking into account both macroscopic behaviour and microscopic interactions. Advances in computing power have enabled more efficient simulations using DEM techniques (Asylbekov et al. 2024; Reineking et al. 2024; Siegmann et al. 2021). Researchers have introduced improved algorithms for faster calculations and increased accuracy in capturing complex phenomena such as

breakage, segregation, and flow patterns within the drum (Ge and Zheng 2024; Ramirez et al. 2024; Zhang et al. 2024). Furthermore, the coupling of DEM with other numerical methods such as Computational Fluid Dynamics (CFD) provides a more comprehensive understanding of particle-fluid interactions (Adhav et al. 2024; Ström et al. 2024; Yao et al. 2020; Zhao et al. 2024). In addition, advances in visualisation techniques have provided more realistic particle motion and system behaviour (Mahboob et al. 2023). In this way, it provides suitable tools for the study of issues such as friction, breakage, and wear. Ansys Fluent DEM©, Ansys Rocky DEM©, Altair DEM© etc. are more widely used software.

In the agricultural industry, peanut grading machines are mostly used to sort by size and ensure consistent quality. However, their performance can be direly affected by friction and wear, leading to reduced productivity, increased maintenance and product damage. To overcome these challenges, researchers frequently use DEM-simulations (Cui et al. 2024), which offer a valuable tool for understanding the complex dynamics in the peanut grading machine. DEM offers various advantages when simulating friction or wear in peanut grading machines: a) Particle level resolution: DEM provides a detailed understanding of particle interactions, allowing friction and wear mechanisms to be accurately characterised. b) Realistic boundary conditions: DEM simulations are able to simulate the real operating environment of peanut grading machines by considering realistic contact and boundary conditions. c) Parametric analysis: DEM allows the study of various operating conditions such as particle size, shape, and material properties, providing information on their influence on friction and wear. Although researchers commonly argue that ML methods should only be applied on experimental data, it is seen that ML can also be performed on simulated data, as well. It may provide shorter prediction time than that of simulations (Bui et al. 2019; Kibriya et al. 2023; Wu et al. 2024; Zhang et al. 2024). Peanut grading machines play a critical role in the agricultural industry by ensuring the quality and efficiency of peanut sizing processes (Akcali et al. 2014). Since wear and friction significantly affect the performance and lifetime of such machines, accurate simulations are necessary to optimize their design and operation. Accuracy also depends on the multi-physics models and assumptions, as well.

Despite significant advancements in time-series prediction techniques, the application of ANFIS for forecasting friction data in peanut kernel drying within rotary drum dryers remains an underexplored area. Existing studies have primarily focused on modeling the drying kinetics, heat and mass transfer mechanisms, and optimization of drying parameters, while limited attention has been given to the dynamic behavior of frictional forces acting on peanut kernels. Friction data is crucial for understanding the mechanical interactions within the drum, which directly influence energy efficiency, product quality, and equipment wear. However, conventional modeling approaches, such as regression-based or purely data-driven machine learning techniques, may lack the interpretability and adaptability required for complex nonlinear systems like rotary drum drying. ANFIS, with its hybrid structure combining neural networks and fuzzy logic, offers a promising alternative, yet its potential for accurate friction prediction in this specific application has not been sufficiently validated. Addressing this research gap could enhance process control strategies, optimize dryer performance, and contribute to the broader goal of automating industrial drying systems through intelligent modeling approaches.

This study aims to simulate using Ansys Rocky DEM© most essentially to the actual conditions and to model the friction data using the ANFIS method, which is a hybrid model. Thus, the effect of wear, which causes significant costs and operational difficulties in the industry, will be better determined. The friction force data from the simulation in a cylindrical sieve are employed. The performance of the ANFIS network is evaluated.

## 2. Materials and Methods

### 2.1. The Net Force Generated in Peanut Kernel Grading

In this study, a peanut grading machine located in Çukurova University Faculty of Agriculture as shown in Figure 1 is simulated. Normal force and coefficient of friction between grain and sieve wall results in friction force (tangential contact force). How to calculate the net force in the tangential direction according to the

domain is explained in this section. Torque can be calculated after the force calculation. Power can be calculated using the torque. Energy is calculated using the power.



**Figure 1.** The peanut grading (sorting, sieving, classification) machine used in the experiments.

To calculate the net force that will be the basis for friction force, equilibrium equations are written for the circular and spiral path as shown in Equation (1) and Equation (2) (Ugurluay and Akcali 2021).

$$F(\beta) = g[\beta(n - \cos\beta) - (n - 1)\sin\beta] - g\mu_d[\beta\sin\beta + (n - 1)(1 - \cos\beta)] - \frac{1}{2}r\mu_d\omega^2\beta^2(1 + n) = 0 \quad (1)$$

$$F(\beta) = \frac{\rho r e}{\beta} \left[ (1 + n(\beta - 1)) \left( g(\cos\varphi - \mu_n \sin\varphi)(\sin\beta - \beta\cos\beta) + \left( g - \frac{1}{2}r\omega^2\beta^2 - g\cos\beta - g\beta\cos\beta \right) \mu_d \right) \right] = 0 \quad (2)$$

where  $\omega$ ,  $r$ ,  $\mu_d$ ,  $\alpha$ , and  $g$  are rotational velocity of the drum, drum's radius, friction coefficient of granular material, rotation angle of the drum, and gravitational acceleration, respectively.  $\beta$  is the angle of the arc swept from bottom of the cylinder.  $e$  is the minimum height of the layer on the drum surfaces.  $n = \frac{h_0}{e}$  and  $h_0$  is the maximum thickness of the layer on the drum surfaces.

## 2.2. Discrete Element Method

The basis of this method is to use equilibrium equations to predict the trajectory of particles. These equations are based on d'Alembert's principle, angular momentum, and Newton's second law of motion. The equilibrium equations are given in Equation (3) and Equation (4). Note that both are ordinary differential equations.

$$m_i \frac{dv_i}{dt} = \sum_j (F_{n,ij} + F_{t,ij}) + m_i g + F_{f \rightarrow p} \quad (3)$$

$$I_i \frac{d\omega_i}{dt} = \sum_j (M_{t,ij} + M_{r,ij}) + M_{f \rightarrow p} \quad (4)$$

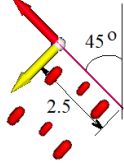
where  $i$ ,  $j$  are the particle number,  $m$  is the mass,  $I$  is the moment of inertia of the particle.  $n$  and  $t$  are the direction vectors in the normal and tangential directions, respectively.  $v$  is the linear velocity vector,  $\omega$  is the rotational velocity vector of the particle.  $F_{f \rightarrow p}$  and  $M_{f \rightarrow p}$  are the force and moment, respectively. Both arises if there is a particle-fluid interaction in the case of CFD-DEM coupling. Since there is no coupling in this study, the expressions for  $F_{f \rightarrow p}$  and  $M_{f \rightarrow p}$  are zero.  $F$  is the force,  $M_{t,ij}$  is the net tangential torque produced by all tangential forces (such as gravity or drag as well as the tangential force component) that cause the particle to rotate.  $M_{r,ij}$  is the rolling resistance torque acting on particle  $i$  by particle  $j$  or the wall. The direction of  $M_{r,ij}$  is the same as that of the rotational velocity, but the sense is opposite. The normal force does not contribute to particle rotation.

Contact occurs as a result of any collision. A contact model is used to calculate the contact forces. Contacts are calculated according to soft or hard sphere techniques. In the hard sphere method, the particles are rigid and there is no deformation in contact. Instead of contact forces, restitution coefficients and shock laws are used to calculate the motion and energy loss during the contact. However, multiple contacts are not allowed. In any collision, forces occur such as Van der Waals forces, liquid bridge forces, and electrostatic forces. In the soft sphere method, although the particles are rigid, the deformation of the particles in contact is calculated using a method called "overlap". In contact, forces that occur without physical contact, such as Van der Waals forces, liquid bridge forces, and electrostatic forces, can also be included in the calculations.

### 2.3. Simulation and Data Collection

Ansys Rocky DEM© software package is used in this study (Rocky 2021). It offers a user-friendly interface and many advanced features. These features are particle shape libraries, different contact detection algorithms, and parallel computing capabilities. The parameters used in the DEM simulation are given in Table 1. The calculation is performed in 60 steps. Each step has a time period of 1 second. In addition, each time period is divided into sub-steps having intervals of 0.1 seconds. 60 seconds of real-time calculation is performed. As a result, a time-dependent friction force dataset consisting of 600 data is obtained.

**Table 1.** Parameters of DEM simulation

Injection properties	Value	
Particle shape	216 polyhedra with triangular faces, 	
Particle type, material	Single component (Peanut kernels)	
Particle material behaviour	Hard sphere	
Particle equivalent diameter distributions, $d_p$ (mm)	22 (100%)+7.6 (22%)	
Particle volume, ( $m^3$ )	5.575e-06	
Particle mass flow rate ( $kg h^{-1}$ )	0.169	
Velocity vector of the particles at the injection point		3 $m s^{-1}$ (normal to the input surface)
Time step size (s)	0.01	
Real time duration (s)	60	
Simulation physics	Value	
Normal force	Linear spring-damper	
Tangential force	Coulomb friction	
Rolling resistance torque	Constant, $\mathbf{M}_{r,ij} = -\mu_r  \mathbf{r}  \times \mathbf{F}_{cn,ij} \frac{\omega_p}{ \omega_p }$	
Numerical softening factor	1	
Gravity ( $m s^{-2}$ )	9.81	
Material properties	Particle	Wall (steel)
Young's modulus, $E$	10.11 MPa	200 GPa
Poisson ratio, $\nu$	0.201	0.3
Solid density, $\rho_s$ ( $kg m^{-3}$ )	416	7850
Bulk density, $\rho_b$ ( $kg m^{-3}$ )	250	--
Drum's rotational speed	--	10 $rev min^{-1}$
Material interaction properties	Particle-particle	Particle-wall
Coefficient of friction, $\mu(\dot{s}_t)_{static}, \mu(\dot{s}_t)_{dynamic}$	0.408, 0.318	0.326, 0.326
Rolling resistance coefficient, $\mu_r$	0.2	0.2
Coefficient of restitution, $\varepsilon$	0.224	0.224

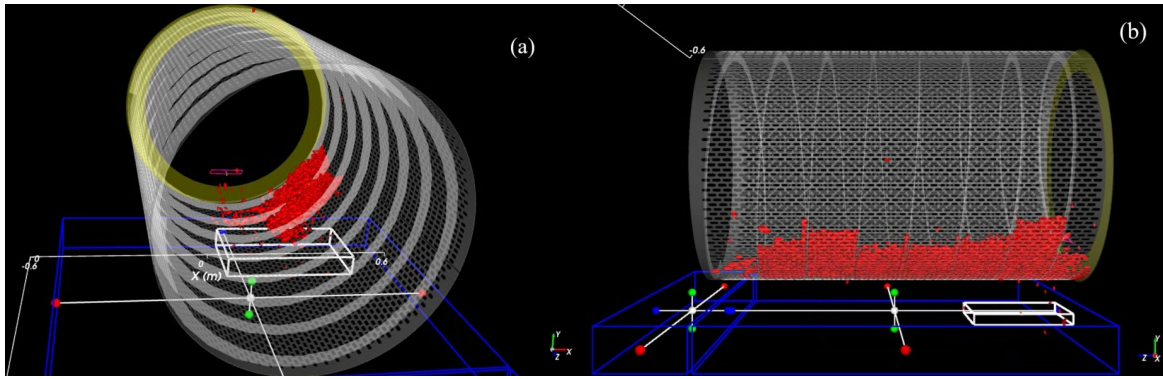


**Figure 2.** DEM based simulation of peanut grading machine and its grading boxes (a) peanut distribution at  $t = 10$  s and (b)  $t = 35$  s

Figure 2 shows the geometry of the screen used in the simulation and screenshots taken at certain time steps. In the images, the flow of the peanut kernels into the domain, the rectangular opening at the inlet, the two accumulation boxes under the screen and the helical structure inside the drum are clearly seen.

Figure 3 shows the time-series data of the calculated friction force. The horizontal axis is the time step. The data are time-dependent friction forces. The elapsed calculation time for a 60-second real-time simulation is 63 days, 18 hours and 27 minutes. The calculations are performed using a computer with 8 GB RAM and a 2.8 GHz quad-core CPU.

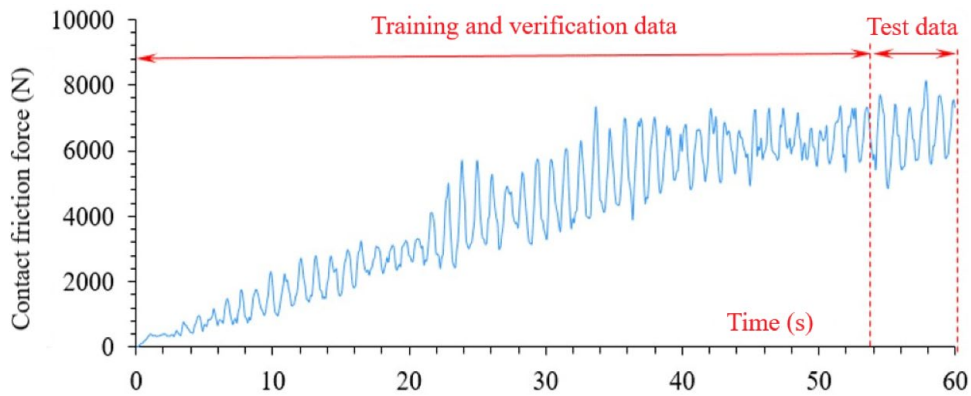


**Figure 3.** Time-series data of the contact friction force and its training/test portions

#### 2.4. Understanding Insight of the Data

Prior to modelling, a critical step is to understand the nature of the time-series data. It helps the selection of hyper-parameters that are good for the data. In time-series analyses, Auto-Correlation (ACF) and Partial Auto-Correlation (PACF) plots are usually examined together to identify time-lags. Also, hypothesis tests can be performed.

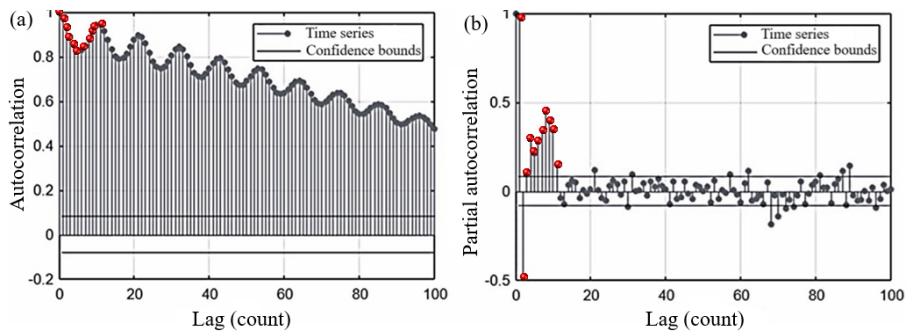


**Figure 4.** For the friction data; (a) ACF, (b) PACF

In Figure 4, ACF and PACF correlograms are given. Both are unitless. Delays are expressed in units of 'time steps'. Each peak in the graph represents one lag. 100 lags are evaluated. A confidence limit of 2 standard deviations is taken as its boundaries. Both graphs show that the data in the series are not randomly distributed, but rather correlated with their lags. It is also observed that the ACF values decrease over time, while the PACF drops suddenly below the confidence limit after the 11<sup>th</sup> lag (white noise). White noise mean the values that have no effect on the lags. Both the gradual decrease in ACF and the sudden drop in PACF indicate that this series has an AutoRegressive (AR) structure with 11 lags, shown AR(11) (Korkmaz and Kacar 2024).

In this study, time-series data representing the variation of friction force over time was utilized. Accordingly, a 11-lag of output was fed as input.

## 2.5. ANFIS

Figure 5 shows the topology of the ANFIS network used.

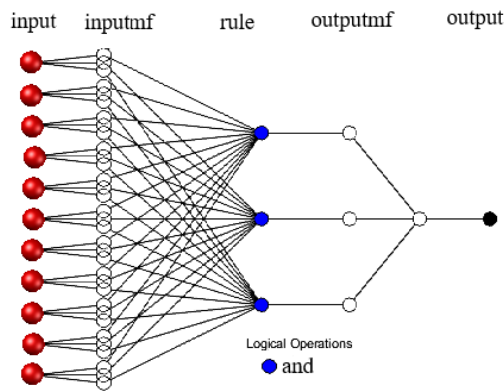


Figure 5. ANFIS network topology

In order to create an ANFIS network, the first stage is to select the hyper-parameters of the network, appropriately. The hyper-parameters are as follows:

- Data partition: Training 90 % (54 s), test 10 % (6 s)
- Number of lags in the data : 11
- Number of inputs :11
- Number of outputs : 1
- Clustering method: Grid Partitioning (Number of clusters: 3, Membership function: Gaussian, output function: Linear (Takagi-Sugeno))
- Maximum number of iterations: 100
- Initial step: 0.01
- Initial acceleration: 0.9
- Initial deceleration: 1.1
- The data were normalised using the formula

$$o(t)^{normalize} = \frac{o(t) - \overline{o(t)}}{\sigma} \quad (5)$$

where,  $o(t)$  is the time-series data at time step  $t$  and  $\overline{o(t)}$  is the mean data and  $\sigma$  is the standard deviation, calculated by

$$\sigma = \sqrt{\frac{\sum_{t=1}^{NN} [(p(t) - \overline{o(t)})]^2}{NN}} \quad (6)$$

$NN$  is the number of total data.  $p(t)$  is the value estimated by the network at time step  $t$ .  $t$  is the time step.

- Error criterion : Mean Square Error,

$$MSE = \frac{1}{NN} \sum_{t=1}^{NN} (p(t) - o(t))^2 \quad (7)$$

- $RMSE$  is Root of  $MSE$ . The unit of  $MSE$  is the square of the unit of the data. Since the friction force data is in unit of Newton ( $N$ ),  $MSE$  will be  $N^2$ . Similarly,  $RMSE$  will be in units of ( $N$ ).

*MAE* is Mean Absolute Error. Its unit is the data unit. *MAPE* is Percentage of *MAE*. *MSE* ( $\text{unit}^2$ ), *RMSE* ( $\text{unit}$ ), *MAE* ( $\text{unit}$ ) and *MAPE* (%) are error metrics used to measure model success. The closer these criteria to zero means the smaller error. Similarly, the closer the *R* (or  $R^2$ ) values to 1 (or  $-1$ ) means the more successful model.

- Correlation coefficient,

$$R = \frac{NN \sum_{t=1}^{NN} p(t)o(t) - (\sum_{t=1}^{NN} p(t))(\sum_{t=1}^{NN} o(t))}{\left(\sqrt{NN \sum_{t=1}^{NN} p(t)^2 - (\sum_{t=1}^{NN} p(t))^2} \sqrt{NN \sum_{t=1}^{NN} o(t)^2 - (\sum_{t=1}^{NN} o(t))^2}\right)} \quad (8)$$

- and the determinant coefficient is  $R^2$ .

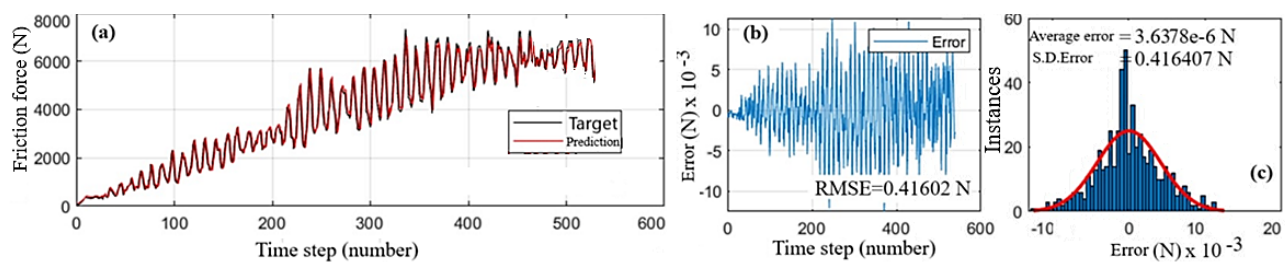
Although the 80/20 training/testing ratio is commonly used in the literature, it is no strict limitation. However, while an insufficient number of samples in the training-set may lead to underfitting, a larger dataset generally has a positive impact on learning performance. In this study, a 90/10 ratio was adopted to ensure better training and to make predictions for the next 6 seconds. This choice is justified by the fact that a total of 60 seconds of friction data was collected, and a 10% data partition is sufficient for a 6-second prediction.

### 3. Results and Discussions

The network's prediction performances are presented in this section. Statistical methods are used in the evaluation of the models.

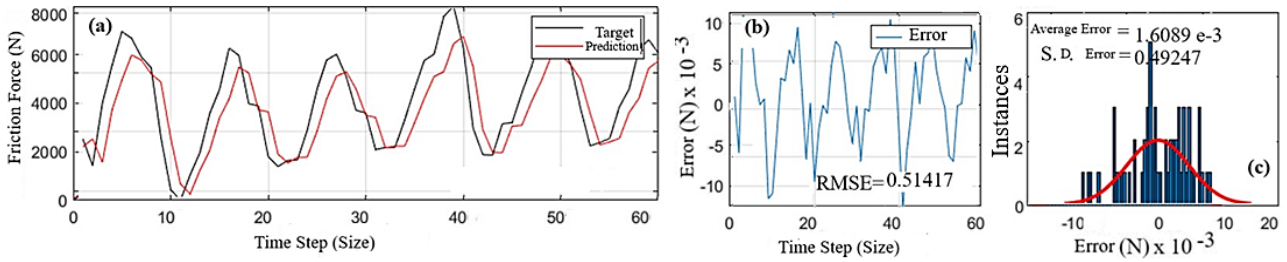
#### 3.1. Prediction Curve and Verification

Figure 6 (a) shows the prediction curve of the ANFIS network on the training data. Although it is seen that the prediction curve given in (a) perfectly passes over the target data, it is seen that there is some error when looking at the error distribution given in (b). RMSE of this difference is given on the figure. The so-called 'target data' is the friction force data obtained from the simulation. (c) shows error histogram where 'average error' indicates the mean error in the histogram, while "S.D. Error" indicates the Standard Deviation of the error. The average error is  $3.6378 \times 10^{-6}$  N, which is very small. The histogram shows a normal distribution. It is desirable to have a bell curve shape in the histograms, which is called 'normal distribution'. The narrowness of this curve indicates that the errors are small. The horizontal axis is the error value. The vertical axis in the histogram is the 'incidence'. Looking at the histogram, it is seen that the highest lines are centred around 'zero error'. It means that small errors occur frequently. In other words, the model predicted well on the training set. This is an expected case because the network is familiar with the data since it is trained with this data. The whole training data had already been used during training, so, the prediction performance was high.



**Figure 6.** (a) Prediction curve on the training data, (b) error distribution and (c) error histogram of the network on the training data

The response curve for the network's prediction on the test data is given in Figure 7 (a), error distribution in (b) and error histogram in (c). This graph makes it possible to analyse only the performance on the test data in more detail. It is noticeable that this model has a high ability to represent peaks and dips, although a constant shift is also present. The performance is lower than that of training performance. It is an expected case because the network has never seen the forecasting data before. Therefore, it has a greater error in prediction. Looking at the histogram, it can be seen that the error frequently goes outside the bell curve. This is an undesirable situation indicating that the error is greater.



**Figure 7.** (a) Prediction curve on the forecasting data, (b) error distribution and (c) error histogram of the network on the test data

The response curve for the prediction of the network on the full data is given in Figure 8 (a), the difference (error) distribution is given in (b) and the difference (error) histogram is given in (c).

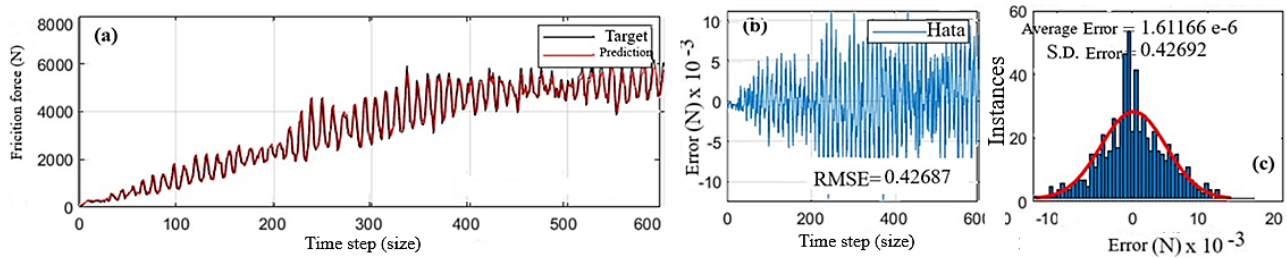


**Figure 8.** (a) Prediction curve on all data set (b) difference (error) distribution and (c) difference (error) histogram of the network on all data

Another frequently-used model performance metric is analysis of variance. One of the basic assumptions of modelling is that the residual has constant variance at all levels. If the model has constant variance, it means that its generalization ability is high. The most common way to determine whether a model has constant variance is to plot the points of model prediction and corresponding residual. If all points are randomly distributed between two parallel lines, then the variance is constant. Otherwise, if the distribution increases or decreases systematically, then the variance is variable. When Figure 9 is analyzed, it can be seen that the variance is homoscedastic (Korkmaz and Kacar 2024). It shows the variance of the model on the test data. The variances in training and validation could also be determined.

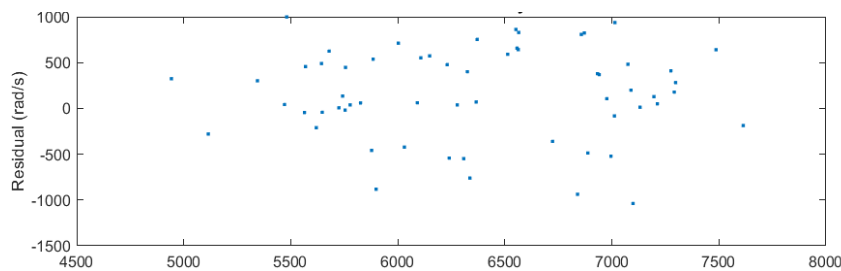


**Figure 9.** Variance analysis

Regression analysis is another technique frequently used in the evaluation of model performance. It gives linear correlation between the prediction of the model and the values in the data set. The correlation coefficient is denoted by  $R$ , while  $R^2$  is called the determinant coefficient. Both are unitless. For  $R$ , values between 0.01-0.29 mean a low level of correlation, 0.3-0.7 means a medium level of correlation, and 0.71-0.99 means a high level of correlation. Zero means no relationship, while negative values mean an inverse relationship. The increase in absolute  $R$  indicates that the relationship becomes more apparent. Figure 10 shows the results of the regression analysis. The horizontal axis is the target while the vertical axis is the predicted values. As expected, the network has the highest correlation on the training data (Figure 10 a). This is because it is very familiar with this data during training. It has recognized this data already. Figure 10-b shows that the network also has a high correlation on the test data. Figure 10-c shows the correlation of the network's prediction on all data. Since the number of data in the training set is much higher, the data points on the graph is also much more. Correlation on the training set is greater than that of test.

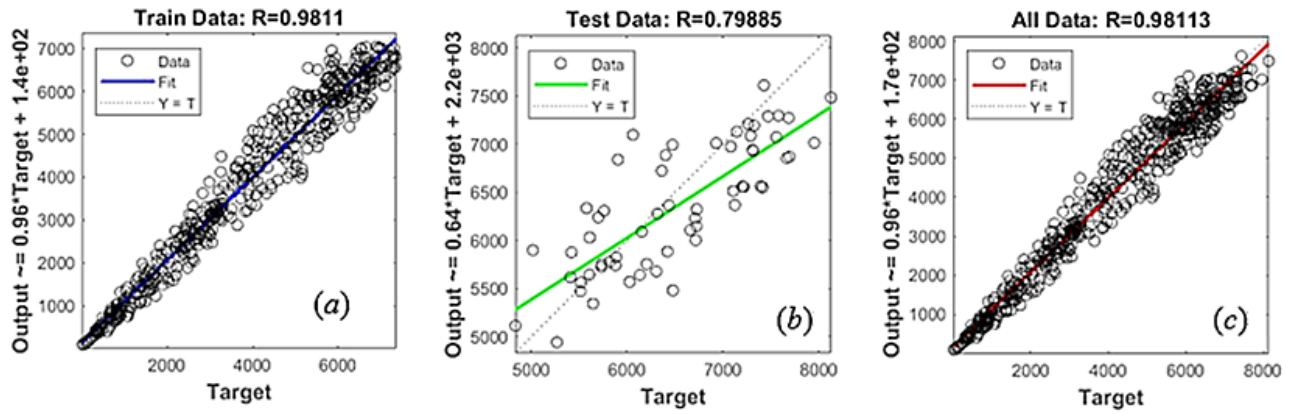


Figure 10. Correlation between the model prediction and (a) training, (b) test, (c) all data

The correlation is 0.799 and RMSE is 0.514 N. MAE is found to be 1.6658%. 100 iterations are performed. The calculations take 20.7 s. There is a high linear relationship between the model outputs and the data set. It is also observed that the ANFIS network eliminates the need for any preprocessing of the data.

Table 2. Indicators recorded during the training of the network

Performance metrics	Values
MAE (unit)*	4.219
MAPE(%)	1.666
Mean Error (unit)	1.61E-03
MSE (unit <sup>2</sup> )	0.264
RMSE (unit)	0.514
Elapsed calculation duration (s)	20.7
$R_{\text{test}}$	0.799
$R_{\text{training}}$	0.981
Iteration number	100

### 3.2. Discussion

ML is rarely used for modelling process parameters in peanut classification whereas curve fitting techniques are more common (Cunha et al. 2024). However, preprocess applied to the data before the curve fitting process disturbs the naturalness of the data to some extent. The generalisation of ANFIS network on the data obtained from Ansys Rocky DEM© simulation is an important motivation for future studies on peanut classification. The most important limitation of DEM simulations is the computational cost. The calculation time increases exponentially as the number of particles in the region increases over time. ML techniques offer reducing these costs. The simulation took 63 days, 18 hours and 27 minutes to calculate the real time of 60 seconds. In the ANFIS method, the total computation time for the 6-second prediction process is 20.7 seconds. When compared, the difference is remarkable. Moreover, no pore-process was applied. The present model has a correlation of 0.799 and an RMSE of 0.514 N. The variance is constant. In addition to general curve shape, peaks-dips could be predicted accurately, as well. Although the terms  $R$  or  $R^2$  are expected to be close to  $\pm 1$ , the use of  $R^2$  provides a more conservative perspective. While the  $R$  value (0.799) indicates a strong correlation, the lower  $R^2$  value (0.638) suggests that the explanatory power of the model is somewhat limited. In this context, despite the low  $R^2$  value, the model can still be considered to have achieved a certain level of success. However, improving the model's performance may require training with a larger dataset and optimizing model parameters. Obtaining more accurate and precise friction and wear data can provide a significant advantage in predicting the lifetime and predictive-maintenance on the grading machines. Recent research shows that DEM-based simulations are an effective method to study these factors in peanut grading machines (Kacar 2023; Korkmaz 2023; Qiao et al. 2024). DEM software provides valuable information on machine design and performance by modelling particle interactions and boundary conditions realistically. With the help of coupled CFD-DEM analysis, the APE (Absolute percentage error) of the ML-

based model for the transitional flow of sand particles was determined as minimum 7.36% and maximum 29.99% (Hu et al. 2024). Hybrid CNN-LSTM hybrid model are applied onto the data obtained from the CFD-DEM simulation of liquid-solid particle mixing and separation in a bi-dispersed fluidised bed. The prediction results are compared with the CFD-DEM results. In terms of computation cost, LSTM takes 2.1-2.5 h and CNN-LSTM takes 6.2-6.5 h while CFD-DEM takes 72-165 h. The best accuracy is obtained from CNN-LSTM in reference with velocity prediction with  $R^2 = 0.86-0.92$ , MAE = 0.0006-0.0046 m s<sup>-1</sup>, RMSE = 0.0030-0.0138 m s<sup>-1</sup> (Xie et al. 2022).

Future work should aim to increase the efficiency, durability and reliability of these machines by improving DEM techniques.

#### 4. Conclusions

This study highlights the potential of using ANFIS for predicting time-series friction data in the peanut grading process. By integrating data obtained from DEM-based simulations, the study demonstrates the feasibility of employing machine learning techniques in agricultural and food processing applications. The findings indicate that ANFIS provides an effective framework for capturing the complex frictional interactions within a rotary drum dryer, offering an efficient alternative to traditional simulation-based approaches.

The significance of this research lies in its contribution to process optimization and automation in industrial drying systems. The results suggest that ANFIS can effectively model and predict friction forces without requiring extensive data preprocessing, thereby reducing computational costs and improving efficiency. This is particularly relevant given the substantial time investment required for high-fidelity DEM simulations, underscoring the necessity of alternative predictive methods that balance accuracy and computational efficiency. The DEM simulation had taken 63 days, 18 hours, and 27 minutes to compute 60 seconds of real-time data. 6 seconds ahead is predicted. The ANFIS method completed both training and forecasting within a total computation time of 20.7 seconds. The remarkable difference between these results is noteworthy.

Future research should focus on enhancing the predictive accuracy and generalizability of the proposed model. Comparative analyses with alternative machine learning techniques, such as deep learning or hybrid approaches, could provide valuable insights into performance improvements. Additionally, incorporating real-world experimental data alongside simulation results could further validate the model's reliability. Investigating the effects of different peanut varieties, processing conditions, and time-series delays may also refine the applicability of the proposed framework. Moreover, integrating external factors such as humidity, temperature, and kernel size distribution into the predictive model could enhance its robustness and practical relevance in industrial applications.

Ultimately, this study serves as a foundation for future advancements in the intelligent modeling of friction forces in food processing systems. By leveraging data-driven methodologies, future research can contribute to the development of more adaptive, efficient, and scalable solutions for agricultural automation and process optimization.

---

**Author Contributions:** Conceptualization, C.K. and İ.K.; methodology, C.K. and İ.K.; software, C.K. and İ.K. ; validation, C.K. and İ.K. ; formal analysis, C.K. and İ.K.; investigation, C.K. and İ.K.; resources, C.K. and İ.K.; data curation, C.K. and İ.K.; writing—original draft preparation, C.K. and İ.K.; writing—review and editing, C.K. and İ.K.; visualization, C.K. and İ.K.; supervision, C.K. and İ.K.; project administration, C.K. and İ.K. All authors have read and agreed to the published version of the manuscript.

**Acknowledgments:** We would like to thank Çukurova University Faculty of Agriculture, Karadeniz Technical University, and Dr. Mehmet Seyhan for providing the opportunity to use Ansys Rocky DEM© for discrete element method simulations and Matlab© for coding the ML method for educational purposes, respectively. We would like to sincerely thank the editors, referees, and contributors for their valuable contributions during this study's review and evaluation phase.

**Conflicts of Interest:** The authors declare no conflict of interest.

---

## References

- Adhav P, Besseron X, Estupinan AA, Peters B (2024). Development and validation of CFD-DEM coupling interface for heat & mass transfer using partitioned coupling approach. *International Communications in Heat and Mass Transfer*, 157: 107801.
- Akcali İD, Mutlu H, Ercan U (2014). Mathematical Model of a Sorting Machine. *Journal of Agricultural Machinery Science*, 10(3): 229-234.
- Asylbekov E, Poggemann L, Dittler A, Nirschl H (2024). Discrete Element Method Simulation of Particulate Material Fracture Behavior on a Stretchable Single Filter Fiber with Additional Gas Flow. *Powders*, 3(3): 367-391.
- Brockwell PJ, Davis RA (2002). *Introduction to time-series and forecasting*: Springer. New York , USA, p.449
- Bui VH, Bui MD, Rutschmann P (2019). Combination of discrete element method and artificial neural network for predicting porosity of gravel-bed river. *Water*, 11(7): 1461.
- Caruana R, Lou Y, Gehrke J, Koch P, Sturm M, Elhadad N (2015). *Intelligible models for healthcare: Predicting pneumonia risk and hospital 30-day readmission*. Paper presented at the Proceedings of the 21th ACM SIGKDD international conference on knowledge discovery and data mining.
- Chen W, Shi K (2021). Multi-scale attention convolutional neural network for time-series classification. *Neural Networks*, 136: 126-140.
- Chou K-Y, Yeh Y-W, Chen Y-T, Cheng Y-M, Chen Y-P (2020). *Adaptive neuro fuzzy inference system based MPPT algorithm applied to photovoltaic systems under partial shading conditions*. Paper presented at the 2020 International Automatic Control Conference (CACCS).
- Cui X, Li X, Du Y, Bao Z, Zhang X, Hao J, Hu Y (2024). Macro-micro numerical analysis of granular materials considering principal stress rotation based on DEM simulation of dynamic hollow cylinder test. *Construction and Building Materials*, 412: 134818.
- Cunha N, da Silva LHM, da Cruz Rodrigues AM (2024). Drying of *Curcuma longa* L. slices by refractance window: Effect of temperature on thermodynamic properties and mass transfer parameters. *Heat and Mass Transfer*, 60(4): 617-626.
- Ge M, Zheng G (2024). Fluid–Solid Mixing Transfer Mechanism and Flow Patterns of the Double-Layered Impeller Stirring Tank by the CFD-DEM Method. *Energies*, 17(7): 1513.
- Hu G, Zhou B, Zheng W, Li C, Wang H (2024). A ML-based drag model for sand particles in transition flow aided by spherical harmonic analysis and resolved CFD-DEM. *Acta Geotechnica*, 20(1):461-474.
- Irshaid M, Abu-Eisheh S (2023). Application of adaptive neuro-fuzzy inference system in modelling home-based trip generation. *Ain Shams Engineering Journal*, 14(11): 102523.
- Jang J-S, Sun C-T (1995). Neuro-fuzzy modeling and control. *Proceedings of the IEEE*, 83(3): 378-406.
- Kacar İ (2023). *Scientific Principles of Mechanical Design and Analysis* (Vol. 381): Academician bookshop.
- Khalaf AH, Lin B, Abdalla AN, Han Z, Xiao Y, Tang J (2024). Enhanced prediction of corrosion rates of pipeline steels using simulated annealing-optimized ANFIS models. *Results in Engineering*, 24: 102853.
- Kibriya G, Orosz Á, Botzheim J, Bagi K (2023). Calibration of micromechanical parameters for the discrete element simulation of a masonry arch using artificial intelligence. *Infrastructures*, 8(4): 64.
- Korkmaz C (2023). The place of organic and organomineral fertilizer production in sustainable agriculture. In A Bayat (Ed.), *Sustainable Agriculture Technologies-II*, Ankara: İKSAD. Vol. 244, pp. 183-205
- Korkmaz C, Kacar İ (2024). Explaining data preprocessing methods for modeling and forecasting with the example of product drying. *Journal of Tekirdag Agricultural Faculty*, 21(2): 482-500.

- LeCun Y, Bengio Y, Hinton G (2015). Deep learning. *Nature*, 521(7553): 436-444.
- Lipton ZC (2015). A Critical Review of Recurrent Neural Networks for Sequence Learning. *arXiv Preprint, CoRR, abs/1506.00019*.
- Mahboob A, Hassanshahi O, Tabrizi AS (2023). Three-dimensional simulation of granular materials by discrete element method (DEM) by considering the fracture effect of particles. *Journal of Civil Engineering Researchers*, 5(2): 14-28.
- Murphy KP (2022). *Probabilistic ML: an introduction*: MIT press, London, England, p:864.
- Pan SJ, Yang Q (2009). A survey on transfer learning. *IEEE Transactions on knowledge and data engineering*, 22(10): 1345-1359.
- Qiao J, Hu K, Yang J, Wang Y, Liu J, Zhou E, . . . Duan C (2024). Research on enhancement of screening performance of a novel drum screen based on the Discrete Element Method simulation. *Powder Technology*, 437: 119567.
- Ramirez CE, Sermet Y, Demir I (2024). HydroCompute: An open-source web-based computational library for hydrology and environmental sciences. *Environmental Modelling & Software*, 175: 106005.
- Reineking L, Fischer J, Mjalled A, Illana E, Wirtz S, Scherer V, Mönnigmann M (2024). Convective drying of wood chips: Accelerating coupled DEM-CFD simulations with parametrized reduced single particle models. *Particuology*, 84: 158-167.
- Rocky DEM© Ansys (2021). DEM technical manual 4.4. 3.
- Siegmann E, Enzinger S, Toson P, Doshi P, Khinast J, Jajcevic D (2021). Massively speeding up DEM simulations of continuous processes using a DEM extrapolation. *Powder Technology*, 390: 442-455.
- Ström H, Luo H, Xiong Q (2024). Perspectives on Particle–Fluid Coupling at Varying Resolution in CFD-DEM Simulations of Thermochemical Biomass Conversion. *Energy & Fuels*, 38(18): 17179-17190.
- Sutton RS (2018). Reinforcement learning: An introduction. *A Bradford Book*. The MIT Press, London, England, p. 548.
- Tien Bui D, Khosravi K, Li S, Shahabi H, Panahi M, Singh VP, . . . Chen W (2018). New hybrids of anfis with several optimization algorithms for flood susceptibility modeling. *Water*, 10(9): 1210.
- Ugurluay S, Akcali ID (2021). Development of a vibrationless sorting system. *Spanish journal of agricultural research*, 19(1): 204.
- Wu W, Chen K, Tsotsas E (2024). Prediction of rod-like particle mixing in rotary drums by three ML methods based on DEM simulation data. *Powder Technology*, 448: 120307.
- Xie Z, Gu X, Shen Y (2022). A ML study of predicting mixing and segregation behaviors in a bidisperse solid–liquid fluidized bed. *Industrial & Engineering Chemistry Research*, 61(24): 8551-8565.
- Yao L, Xiao Z, Liu J, Zhang Q, Wang M (2020). An optimized CFD-DEM method for fluid-particle coupling dynamics analysis. *International Journal of Mechanical Sciences*, 174: 105503.
- Zhang C, Chen Y, Wang Y, Bai Q (2024). Discrete element method simulation of granular materials considering particle breakage in geotechnical and mining engineering: A short review. *Green and Smart Mining Engineering*, 1(2): 190-207.
- Zhang T, Li S, Yang H, Zhang F (2024). Prediction of constrained modulus for granular soil using 3D discrete element method and convolutional neural networks. *Journal of Rock Mechanics and Geotechnical Engineering*, 16(11): 4769-4781.
- Zhang Y, Cao Z, Liu C, Huang H (2024). Fluid-solid coupling numerical simulation of micro-disturbance grouting treatment for excessive deformation of shield tunnel. *Underground Space*, 19:87-100.

- Zhao Z, Zhou L, Bai L, Wang B, Agarwal R (2024). Recent advances and perspectives of CFD–DEM simulation in fluidized bed. *Archives of Computational Methods in Engineering*, 31(2): 871-918.
- Zhou L, Wang B, Cao Y, Zhao Z, Agarwal R (2024). Fluidisation of spherocylindrical particles: computational fluid dynamics–Discrete element method simulation and experimental investigation. *Engineering Applications of Computational Fluid Mechanics*, 18(1): 2297537.